Quantitative description of disorder parameters in (GaIn)(NAs) quantum wells from the temperature-dependent photoluminescence spectroscopy

O. Rubel[a)]
Department of Physics and Material Sciences Center, Philipps-University Marburg,
Marburg D-35032, Germany

M. Galluppi
Infineon Technologies AG, Corporate Research Photonics, Munich D-81730, Germany

S. D. Baranovskii and K. Volz
Department of Physics and Material Sciences Center, Philipps-University Marburg,
Marburg D-35032, Germany

L. Geelhaar and H. Riechert
Infineon Technologies AG, Corporate Research Photonics, Munich D-81730, Germany

P. Thomas and W. Stolz
Department of Physics and Material Sciences Center, Philipps-University Marburg,
Marburg D-35032, Germany

Photoluminescence in (GaIn)(NAs) quantum wells designed for laser emission was studied experimentally and theoretically. The observed temperature dependences of the luminescence Stokes shift and of the spectral linewidth evidence the essential role of disorder in the dynamics of the recombining excitations. The spatial and energy disorders can cause a localization of photocreated excitations supposedly in the form of excitons. Theoretical study of the exciton dynamics is performed via kinetic Monte Carlo simulations of exciton hopping and recombination in the manifold of localized states. Direct comparison between experimental spectra and theoretical calculations provides *quantitative* information on the energy scale of the potential fluctuations in (GaIn)(NAs) quantum wells. The results enable one to quantify the impact of annealing on the concentration of localized states and/or on the localization length of excitons in (GaIn)(NAs) quantum wells. © *2005 American Institute of Physics.* [DOI: 10.1063/1.2058192]

I. INTRODUCTION

Recent progress in the development of laser diodes operating in the range of wavelengths between 1.3 and 1.55 μm became possible due to incorporation of high amounts of In and N into GaAs.[1] Being grown at extreme nonequilibrium conditions such heterostructures inevitably posses a certain degree of disorder due to their alloy structure and/or imperfect interfaces.[2,3] The energy disorder gives rise to carrier localization that dramatically affects optical properties.[3] Measurements of the photoluminescence (PL) response has become a standard tool for characterizing the quality of the samples, in particular for revealing the disorder energy scale. The PL peak energy and the PL linewidth in (GaIn)(NAs) quantum wells (QW's) demonstrate nonmonotonous temperature dependences[2–5] shown schematically in Fig. 1. The main experimentally observed trends of *T*-dependent PL spectra in (GaIn)(NAs) QW's are (i) an anomalous redshift of the PL peak energy in the range of intermediate temperatures, the so-called *S*-shape behavior; (ii) a peak of the PL linewidth within a narrow temperature range. These features of the PL spectra suggest an essential role of disorder in carrier dynamics.[6–10]
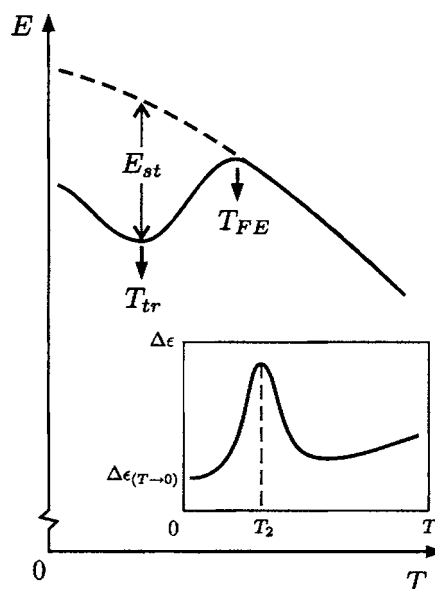
FIG. 1. Schematic shapes of the *T*-dependent PL peak position (solid line) and the band-gap variation with temperature (dashed line). The deviation between the PL peak energy and the band gap for the temperatures below T_{FE} is attributed to emission from localized excitonic states. The insert depicts the typical *T*-dependence of the PL linewidth.

a)Electronic mail: Oleg.Rubel@Physik.Uni-Marburg.de

98, 063518-1

The experimentally observed effects of disorder on the dynamics of recombining carriers can be reproduced within a model where spatially localized excitons hop between localized states distributed randomly in space and energy. A comparison between experimental data and simulation results can provide valuable information on disorder parameters of the studied heterostructures, such as the energy scale and the shape of the band tail as well as the density of localized states and the localization length of an exciton center-of-mass. A kinetic Monte Carlo simulation of PL spectra based on a phenomenological hopping model and the algorithm developed in Ref. 10 was recently applied in order to explain *T*-dependences of PL spectra in (GaIn)(NAs)/GaAs QW's,[11] (ZnCd)Se quantum islands,[12] and (InGa)N/GaN QW's.[13] The comparison between theory and experiment makes sense only if the simulations are carried out for particular material parameters typical for heterostructures studied experimentally.

In this paper we present an experimental and theoretical study of *T*-dependent PL spectra in (GaIn)(NAs) QW's designed for the laser application. Experimental data are interpreted within the model quoted above. The simulations were performed using a set of material parameters appropriate for (GaIn)(NAs) QW's. The characteristic energy scale of the disorder potential is quantified via comparison between simulation results and experimental data for (GaIn)(NAs) QW's including numerous previous studies available in the literature. In addition, we quantify the impact of annealing on the concentration of localized states and/or on the localization length of excitons in (GaIn)(NAs) QW's.

II. THEORETICAL MODEL

In order to study the hopping energy relaxation and luminescence of localized correlated electron-hole pairs in the form of excitons, we employ the kinetic Monte Carlo algorithm suggested in Ref. 10. At sufficiently low temperatures, electrons and holes generated after optical excitation are captured as excitons into localized states and their center-of-mass can perform transitions between localized states in the band tail. These phonon-assisted transitions are described by Miller-Abrahams tunnelling rates.[14] The hopping transition rate from an occupied site i to an empty site j over a distance r_{ij} is given by

$$\nu_{ij} = \nu_0 \exp\left(-\frac{2r_{ij}}{\alpha} - \frac{E_j - E_i + |E_j - E_i|}{2k_B T}\right), \quad (1)$$

where E_i and E_j are the energies of sites i and j, respectively, T is the lattice temperature, k_B is Bolzmann's constant, α is the decay length of the localized exciton center-of-mass wave function, and ν_0 is the attempt-to-escape frequency. Being confined by the QW barriers, excitons can move only in the plane of the QW, which reduces the problem to two spatial dimensions.

Being randomly distributed in two-dimensional space with some density N_0, the localized states also have a certain energy distribution forming the band tail. The energy distribution of localized states can be expressed in the general form

TABLE I. Chemical compositions of the QW's and the Varshni parameters for the temperature-dependent band gap $E_g(T) = E(0) - aT^2/(T+b)$.

Sample	x_{In}, %	y_N, %	$E(0)$, eV	a, eV K^{-1}	b, K
A-as gr.	38	1.6	0.9581	4.2×10^{-4}	240
A-ann.	38	1.6	0.9849	4.2×10^{-4}	200
B-as gr.	30	1.6	1.0550	4.2×10^{-4}	180
B-ann.	30	1.6	1.0641	4.2×10^{-4}	200

$$g(E) = \frac{N_0}{E_0} f(E/E_0), \quad (2)$$

where E_0 is the characteristic energy scale and $f(E/E_0)$ is a function that represents the shape of the band tail. Finding the shape and the energy scale of this density of states (DOS) is of high interest for the characterization of the quality of heterostructures. In our model we consider the case of uncorrelated disorder in the sense that energies of localized states do not depend on their spatial positions.

We restrict our consideration to hopping and recombination of mutually independent excitons. This corresponds to the experimental situation where the excitation rate is sufficiently low and excitons relax independently from each other. Hopping and recombination of a large number of excitons are simulated. The fate of each exciton is determined in the following way. The exciton decay rate at site i is defined as the sum of the radiative recombination rate τ_0^{-1} and the total hopping rate $\Sigma_j \nu_{ij}$, where the summation index j runs over all possible target states. We assume for simplicity that the radiative recombination rate τ_0^{-1} does not depend on temperature and energy E. A random number from a uniform distribution is used in order to specify the outcome of a Monte Carlo step: it is either exciton transfer to another localized state in the band tail or exciton recombination. In the latter case the energy position of the exciton is stored. The PL spectrum is constructed from the distribution of energies of recombined excitons. A comprehensive description of the algorithm can be found in Ref. 10.

The set of parameters of the model (ν_0, α, E_0, N_0, τ_0, and T) can be combined into only three dimensionless parameters: $\nu_0\tau_0$, $N_0\alpha^2$, and $k_B T/E_0$. For the sake of generality, we present and analyze our theoretical results in terms of these dimensionless parameters.

III. EXPERIMENTAL DETAILS

Samples were grown by solid-source molecular-beam epitaxy on semi-insulating (001) GaAs substrates. Nitrogen was supplied by a rf plasma source. The structure of the samples contains a 6.5-nm-thick $Ga_{1-x}In_xN_{0.016}As_{0.984}$ single QW that is surrounded on both sides by 200 nm GaAs barriers followed by a 15-nm-thick AlAs/GaAs superlattice. In the paper we present the results for two different samples: "A" grown at 400 °C with an indium content of 38% and "B" grown at 430 °C with an indium content of 30% (see Table I). Both samples were annealed in hydrogen atmosphere at 720 °C for 30 min.

The PL measurements were performed at temperatures between 15 and 300 K in a closed-cycle-He cryostat. The
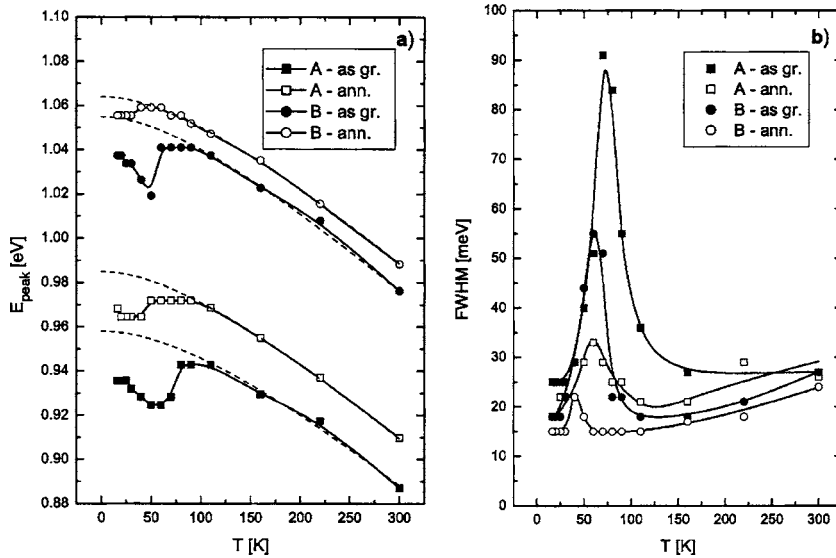
FIG. 2. Experimental results for the PL peak position (a) and the PL linewidth (b) as a function of temperature for a series of samples with (GaIn)(NAs)/GaAs QW's. The filled and open symbols correspond to results taken from as-grown and annealed samples, respectively. The dashed curves on panel (a) show the band-gap variation with temperature obtained by the Varshni fit with the parameters listed in Table I. The solid lines are guides to the eye.

samples were excited continuously by a He–Ne laser (λ = 633 nm) with a power density of about 300 W/cm^2. The PL was dispersed by a single 1 m monochromator and detected by a liquid N$_2$-cooled Ge detector.

The nominal In and N composition was determined on ternary reference samples combining analysis of high-resolution x-ray diffraction and transmission electron microscopy measurements with precalibrated PL data.

IV. RESULTS AND DISCUSSION

A. Experimental results

The experimental temperature dependences of the PL peak energy position and of the PL linewidth for samples A and B as grown and after the annealing process are shown in Fig. 2. These data are in line with the schematic trends sketched in Fig. 1. Both samples show signatures of localization at low temperatures. Deviation of the experimental points for the PL peak energy from the corresponding Varshni behavior of the energy gap in Fig. 2(a) clearly suggests emission from localized states. The samples demonstrate a nonmonotonous temperature dependence of the Stokes shift known as S-shape. The remarkable observation is that the maximum value of the Stokes shift is correlated with the temperature T_{tr} corresponding to the local minimum of the PL peak energy as a function of temperature. The samples with higher values of the Stokes shift have higher temperatures T_{tr}.

The full width at half maximum (FWHM) of the PL spectra in Fig. 2(b) also reveals a nonmonotonous T-dependence with the trend sketched in the insert of Fig. 1. The PL linewidth has a pronounced peak in a rather narrow temperature range. Although the temperature T_2, at which the linewidth has its maximum value, and the low-temperature PL linewidth $\Delta\epsilon_{(T=15\ K)}$ are individual for each sample, experimental data for different samples in Fig. 2(b) suggest a strong correlation between these two characteristics. Moreover, there is a correlation between striking properties of the T-dependent PL peak energy and the PL linewidth in Fig. 2. Apparently, the deeper is the Stokes shift, the higher is the

temperature T_{tr}, the broader is the PL spectrum, the higher is the temperature T_2. This scaling behavior will be used below in order to quantify the energy scale E_0 of the disorder potential.

Appreciable changes in the PL properties of samples are induced by annealing. Although the general trends of the T-dependent PL remain unaffected by annealing, they look less pronounced than in as-grown samples. The S-shape behavior for annealed samples is not as developed as for as-grown samples and it seems to be affected by the indium concentration and/or by the growth temperature; the PL linewidth also decreases due to annealing and the characteristic temperature T_2 shifts towards lower temperatures. Our observations for the annealing-induced changes in the PL characteristics are in line with those discussed by other groups, see, e.g., Ref. 5.

In the following, it is important to keep in mind that characteristic energies of the PL spectra scale with disorder parameter E_0 of the DOS in Eq. (2). One of our goals is to establish the proportionality factors between PL characteristics and E_0.

B. Choice of model parameters

Before performing the simulation of the PL spectra one should identify the range of parameters $\nu_0\tau_0$ and $N_0\alpha^2$ appropriate for (GaIn)(NAs) QW's. The attempt-to-escape frequency ν_0 is usually assumed to be of the order of Debye frequency 10^{13} s^{-1}. The lifetime of excitons in (GaIn)(NAs) QW's estimated from time-resolved PL measurements is approximately 1 ns.[15,16] Therefore, the product $\nu_0\tau_0$ is of the order 10^4. The concentration of localized states, N_0, and the carrier localization radius, α, essentially depend on many factors, such as the chemical composition, growth conditions, a postgrowth treatment, etc. Although the overlap parameter $N_0\alpha^2$ is an adjustable parameter in our model, we can consider the value $N_0\alpha^2=1$ as the upper limit that allows us to treat the shallow states of the band tail as localized ones. It is appropriate to take $N_0\alpha^2=0.1$ as the lower limit for a dilute system in which the exciton dynamics is almost suppressed due to the weak coupling between localized states.
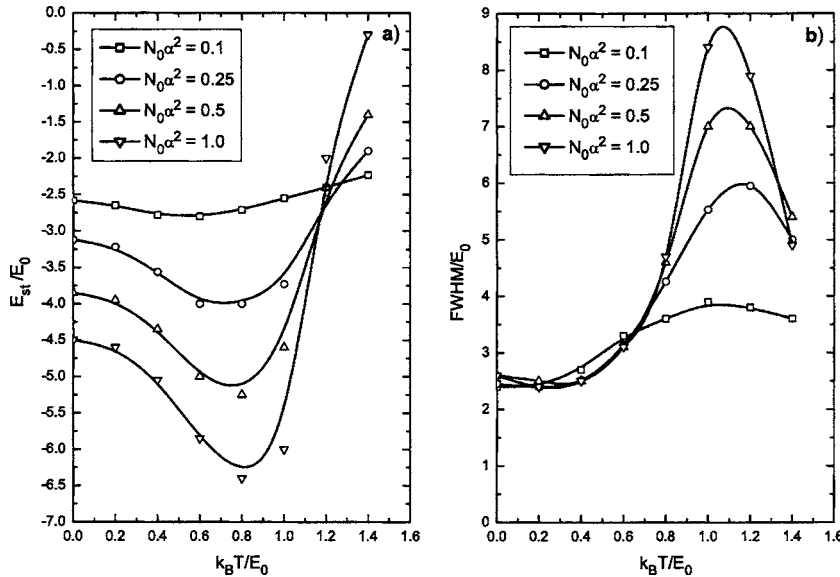
FIG. 3. Simulated PL Stokes shift (a) and the PL linewidth (b) as a function of temperature obtained for different values of the overlap parameters $N_0\alpha^2$ taking the fixed parameter $\nu_0\tau_0=10^4$.

The crucial characteristics of the system is the shape of the band tail caused by the disorder potential. It is commonly accepted that the band tail in diluted nitride semiconductors can be described by the exponential function[17]

$$g(E) = \frac{N_0}{E_0} \exp\left(\frac{E}{E_0}\right), \tag{3}$$

with some characteristic energy scale E_0. The reason for that is the exponential low-energy tail of low-temperature PL spectra. An additional argument in favor of the exponential form of the band tail can be drawn from the comparison between the experimental results for the T-dependent PL linewidth and the simulation results for different forms of the band tail obtained recently in Ref. 11. According to the simulation results, the T-dependent PL linewidth in the exponential DOS demonstrates the peak at $T \approx E_0/k_B$. If, however, one takes a stronger energy-dependent DOS, for example, a Gaussian one with the energy scale E_0', the linewidth increases with rising temperatures until $T \approx 0.8E_0'/k_B$ and then *saturates*. Experimental data for the linewidth in Fig. 2(b) clearly show a maximum at the temperature labeled in Fig. 1 as T_2 indicating the validity of the exponential DOS in our samples. It is remarkable that such a T-dependence of the PL linewidth is not a unique property of the samples studied here, but it is a rather general feature commonly observed in Ga(NAs) and (GaIn)(NAs) QW's.[17]

C. Simulation results

Let us consider the simulation results for the Stokes shift E_{st} and the FWHM $\Delta\epsilon$. These characteristics were derived directly from simulated PL spectra in contrast to the previous studies[11,12] where the average value of the PL energy was treated as a PL peak and the standard deviation was used for the linewidth. When interpreting the simulation results, we define the Stokes shift as the difference between the PL peak energy and the origin of the energy axis in Eq. (3). In the experiment, however, the Stokes shift is usually attributed to the difference between the PL excitation energy and the PL peak energy. Since we will not consider below the magnitude

of the Stokes shift, this discrepancy in the definitions is not essential for the consideration below. Only the temperature T_{tr} corresponding to the minimal energy of the PL peak will be used for quantitative comparsion between theory and experiment. This temperature does not depend on the reference energy for the definition of the Stokes shift.

The simulated results for the PL Stokes shift and the PL linewidth (FWHM) are shown in Fig. 3 as a function of temperature for different values of the overlap parameter $N_0\alpha^2$. When analyzing T-dependent PL characteristics, the temperature scale is traditionally divided into three ranges.[17] At low temperatures ($T \ll E_0/k_B$) the PL is governed by recombination of localized excitons. At intermediate temperatures ($T \approx E_0/k_B$) thermally induced transitions of excitons from deep to shallow states in the band tail can take place. At high temperatures ($T \gg E_0/k_B$) recombination of delocalized excitons is believed to dominate the PL spectrum. We shall discuss our simulation results in terms of this classification.

1. Low temperature ($T \ll E_0/k_B$)

In the limit $T \to 0$ the hopping transitions proceed only downward in energy. This regime is usually called the energy-loss hopping. Being trapped after the photogeneration, excitons usually perform several hops until the time for the next hop becomes comparable to the exciton lifetime τ_0. In every hopping transition the exciton loses in average the energy E_0. Such dynamics gives rise to an essential redshift of the spectral line with respect to the band gap, the so-called Stokes shift. The values of the Stokes shift in Fig. 3(a) range between $2.5E_0$ and $4.5E_0$ depending on the value of the overlap parameter $N_0\alpha^2$. The higher values of the Stokes shift correspond to the higher values of the overlap parameter $N_0\alpha^2$. Despite the difference in the PL peak energies for the different values $N_0\alpha^2$, the linewidth at $T \to 0$ is close to the value $2.5E_0$ for various $N_0\alpha^2$'s [Fig. 3(b)].

2. Intermediate temperature ($T \approx E_0/k_B$)

When the temperature increases, upward hops in energy become also possible. Therefore, excitons have a chance to

explore more sites and to find energetically deeper states for recombination. This explains the anomalous shift of the PL peak energy toward lower energies when the temperature increases up to the value $T_{tr} \approx 0.7E_0/k_B$ [Fig. 3(a)]. This effect is more pronounced for the samples with enhanced coupling between localized states, i.e., for the higher values of the parameter $N_0\alpha^2$. When the temperature approaches the value $T \approx E_0/k_B$, the energy relaxation mechanism changes from the energy-loss hopping to the one similar to the multiple-trapping regime.[10] This results in the blueshift of the PL peak energy and in the increase of the PL linewidth. The PL linewidth approaches its maximum at the temperature $T_2 \approx 1.1E_0/k_B$ [Fig. 3(b)]. It is remarkable that the maximum value of the linewidth essentially depends on the parameter $N_0\alpha^2$, whereas the transient temperature T_2 does not.

3. High temperature ($T \gg E_0/k_B$)

The further increasing of temperature brings excitons to an equilibrium energy distribution. At sufficiently high temperatures, the energy distribution of excitons tends to reproduce the DOS. Under such circumstances the PL spectrum shrinks again and the PL peak energy increases (Fig. 3). The energy distribution of excitons at the temperature above T_{FE} in Fig. 1 is fully thermalized and the Stokes shift becomes negligibly small. Some researchers associate this regime with delocalization of excitons.[5] Since in our model only localized excitons contribute to the PL spectrum, we restrict our analysis taking the temperatures below $1.4E_0/k_B$ when localized excitons dominate the PL spectra. Although we cannot give a theoretical estimate for the delocalization temperature T_{FE}, we can predict that T_{FE} depends not solely on E_0, but it is also sensitive to the coupling between localized states and to the lifetime of excitons (parameters $N_0\alpha^2$ and $\nu_0\tau_0$, respectively). Comparing the results for the Stokes shift at $N_0\alpha^2 = 1.0$ and $N_0\alpha^2 = 0.1$ in Fig. 3, one can conclude that excitons in the sample with the high overlap parameter almost approached an equilibrium distribution ($E_{st} \to 0$) at the temperature $1.4E_0/k_B$, whereas in the case of low coupling between localized states the exciton population nevertheless remains nonequilibrium at this temperature.

In order to illustrate our model, let us compare the experimentally observed transient temperature T_{tr} with that simulated in our model. It is known from independent estimates that the characteristic energy of the band tail in (GaIn)(NAs) QW's is of the order of $E_0 \approx 9$ meV.[11,15] The transient temperature can therefore be estimated as $T_{tr} \approx 0.7E_0/k_B = 73$ K. This temperature is in agreement with numerous experimental data on (GaIn)(NAs) QW's where the maximum of the Stokes shift usually occurs between 40 and 110 K,[2–5,18] depending on the chemical composition and growth conditions.

D. Characteristic energy scale

In order to identify the DOS energy scale, E_0, from a comparison between simulated PL spectra and experimental data, one needs to find such PL characteristic features which are sensitive to E_0 and do not depend (or very weakly depend) on other parameters, such as $N_0\alpha^2$ and $\nu_0\tau_0$. Compre-

TABLE II. Relations between the characteristic energy scale, E_0, and some PL characteristics pointed out in Fig. 1.

Characteristic	Notation	Value
T of max. Stokes shift	T_{tr}	$(0.6–0.8)E_0/k_B$
T of max. PL linewidth	T_2	$(1.0–1.2)E_0/k_B$
FWHM of PL spectrum at low T	$\Delta\epsilon_{(T\to 0)}$	$\approx 2.5E_0$

hensive analysis of the simulated results for the PL peak energy and the PL linewidth shown in Fig. 3 evidences that temperature of the maximum Stokes shift, T_{tr}, the temperature of the maximum PL linewidth, T_2, and the FWHM at low temperature, $\Delta\epsilon_{(T\to 0)}$, are the best candidates to quantify E_0. We present these characteristics in Table II along with the corresponding relations to E_0.

The relations between T-dependent features of PL spectra and the characteristic energy of the band tail, E_0, in Table II provide three independent ways to determine E_0. Table III summarizes the results for E_0's extracted from experimental data in Fig. 2 as well as those from numerous previous studies of the T-dependent PL spectra of (GaIn)(NAs) QW's. The results for E_0 in Table III are gathered in three columns according to the PL characteristics used in order to extract E_0. The lack of some numbers in Table III is due to lack of experimental results for the corresponding PL characteristics. In the ideal case, the characteristic energies E_0, estimated in different ways, should match each other. However, the values E_0 derived from the PL linewidth at low temperature (fourth column in Table III) are slightly higher than the estimates based upon the temperature of maximum Stokes shift, T_{tr}, and the temperature of maximum PL linewidth, T_2. The reason might be related to some additional factors which cause the low-temperature broadening of the PL spectra. For example, the disorder that influences electrons and holes separately might contribute to the line broadening, while we consider in the simulation only the disorder affecting the exciton center-of-mass. When determining E_0 from the temperature T_{tr} corresponding to the maximum Stokes shift, the accuracy is mostly limited by the dispersion of experimental data for the PL peak energy and for the width of the band gap. Therefore, we suspect that the most accurate estimates for the characteristic energy scale E_0 might be obtained from the temperature of maximum PL linewidth, T_2.

The characteristic energies E_0 for various (GaIn)(NAs) QW's quoted in Table III range between 3 and 15 meV depending on their chemical compositions, growth techniques, and postgrowth treatments. The estimates for E_0 based on simply fitting the low-energy tail of low-temperature PL spectra to an exponential function[17,19] $I(E) \propto \exp(E/E_0)$ result in higher values of E_0 being in the range between 6 and 14 meV for the samples studied here. Other researchers[17,19] reported even higher values of E_0 between 30 and 50 meV extracted in the same manner. In order to check the validity of this approach, we fitted the low-energy tail of the simulated PL spectra to an exponential function. The value of the characteristic energy extracted from such a fit reproduces the nominal value E_0, used to generate a PL spectrum. The rea-

TABLE III. Characteristic energy of the band tail, E_0 (meV), for various (GaIn)(NAs) samples extracted from PL spectra by using relations in Table II. The values in brackets refer to the corresponding PL characteristics: T_{tr} is the temperature of maximum Stokes shift, T_2 is the temperature of maximum PL linewidth, and $\Delta\epsilon_{(T\to 0)}$ is the FWHM of PL spectrum at low temperatures.

Sample	E_0 (T_{tr}, K)	E_0 (T_2, K)	E_0 $(\Delta\epsilon_{(T\to 0)}, meV)$	Reference
A (as grown)	6–9 (60)	5–6 (70)	10 (25)	Present study
A (annealed)	4–6 (40)	4–5 (60)	7 (18)	Present study
B (as grown)	5–7 (50)	4–5 (60)	7 (18)	Present study
B (annealed)	3–4 (30)	3 (40)	6 (15)	Present study
$Ga_{0.69}In_{0.31}N_{0.006}As_{0.994}$ (as gr.)	6–9 (60)	6–8 (90)	8 (19)	4
$Ga_{0.69}In_{0.31}N_{0.009}As_{0.991}$ (as gr.)	4–6 (40)	5–6 (70)	10 (24)	4
S135 (annealed at 900 °C, 15 s)[a]	8–11 (73)	⋯	14 (35)	5
S199 (annealed at 850 °C, 15 s)[b]	5–7 (51)	⋯	9 (22)	5
S200 (as grown)[c]	8–11 (74)	⋯	11 (27)	5
S200 (annealed at 800 °C, 15 s)[d]	6–8 (57)	⋯	10 (25)	5
$Ga_{0.72}In_{0.28}N_{0.028}As_{0.972}$ (as gr.)	12–16 (110)	⋯	⋯	2
$Ga_{0.72}In_{0.28}N_{0.028}As_{0.972}$ (ann.)	10–13 (90)	⋯	⋯	2
$Ga_{0.69}In_{0.31}N_{0.045}As_{0.955}$ (as gr.)	⋯	9–10 (120)	11 (27)	3
$Ga_{0.62}In_{0.38}N_{0.03}As_{0.97}$−A (ann.)	9–11 (80)	⋯	⋯	18
$Ga_{0.75}In_{0.25}N_{0.025}As_{0.975}$ (ann.)	⋯	6–7 (80)	⋯	26
$Ga_{0.63}In_{0.37}N_{0.01}As_{0.99}$ (ann.)	6–9 (60)	9–10 (120)	12 (30)	11

[a]PL peak energy at 19 K: E_p=0.92 eV.
[b]E_p=0.87 eV.
[c]E_p=0.76 eV.
[d]E_p=0.85 eV.

son for the discrepancy between E_0's determined from T-dependent PL characteristics and from low-energy tail of PL spectra remains unclear.

The postgrowth annealing step has a significant impact on the optical emission of (GaIn)(NAs) QW's.[5,20] Reduction of the Stokes shift along with the narrowing of the PL linewidth, experimentally observed in annealed samples, evidences that annealing affects the potential fluctuations responsible for exciton localization. So far, the effect of annealing on the potential fluctuations was discussed in the literature mainly qualitatively. Our estimates in Table III, however, provide *quantitative* data for the characteristic energies of as-grown and annealed samples. According to the estimates, the characteristic energy E_0 decreases by approximately 20% for annealed samples in comparison with E_0 values for as-grown samples. This can be attributed to the improvement of the crystal quality in annealed samples that results in smoothing the compositional fluctuations,[21,22] changes in nitrogen local environment,[23] and dissolution of nitrogen complexes observed in as-grown samples.[24,25]

Along with decreasing the disorder energy scale E_0, annealing can induce some changes in the concentration of localized states, N_0, and/or in the localization length α. Annealing-induced reduction in the absolute value of the Stokes shift and in the maximum PL linewidth in Fig. 2 cannot be explained solely by changes in the magnitude of E_0 discussed in the previous paragraph. Additional modification of the parameter $N_0\alpha^2$ is required in order to account for the experimental data. Simulation results in Fig. 3(b) show that the ratio between the maximum PL linewidth and the disorder energy scale, $\Delta\epsilon_{(T_2)}/E_0$, is extremely sensitive to the value of the overlap parameter $N_0\alpha^2$. This ratio can lie within the range between 4 and 9 depending on the value $N_0\alpha^2$. Combining experimental data for the PL linewidth in Fig.

2(b) with extracted values E_0 in Table III, one evaluates the change in the ratio $\Delta\epsilon_{(T_2)}/E_0$ from approximately 8.5±0.5 to 4.5±0.5 for as-grown and annealed samples, respectively. Straightforward analysis yields the value $N_0\alpha^2\simeq 1$ for as-grown samples and the value $N_0\alpha^2\lesssim 0.25$ for annealed ones. This means that either the concentration of localized states decreases by a factor of 4 or the localization length decreases by a factor of 2 due to the effect of annealing. Also a simultaneous changes in N_0 and α induced by annealing cannot be excluded. This result is new for the optical characterization of annealing effects in (GaIn) (NAs) QW's, however, its microscopic mechanism still needs to be clarified.

Annealing-induced changes in absolute values of the Stokes shift can also be interpreted in a similar manner, though additional information on the excitation spectra is required. When doing that, one should take into account that the Stokes shift, though scaling with E_0, also essentially depends on the concentration of localized states accounted in the parameter $N_0\alpha^2$ [see Fig. 3(a)].

V. CONCLUSIONS

Experimental evidences of the correlation between the disorder energy scale and the PL characteristics such as the temperature corresponding to the maximum Stokes shift, the temperature corresponding to the maximum PL linewidth, and the linewidth of the PL spectrum at low temperatures were observed in a series of (GaIn) (NAs) QW's. A kinetic Monte Carlo simulation of hopping energy relaxation of excitons was performed in order to establish proportionality factors between the disorder energy scale E_0 and the characteristics of the PL spectra. The theoretical results were applied to a variety of experimental data in order to evaluate the values of E_0 in (GaIn) (NAs) QW's. It was shown that

the band tail in (GaIn) (NAs) QW's has the exponential form with the energy scale E_0 in the range between 4 and 14 meV depending on their chemical compositions, growth techniques, and postgrowth treatments. The postgrowth annealing reduces the corresponding values of E_0 by approximately 20% in comparison with as-grown samples. We extended interpretation of S-shape dependences beyond traditional estimates for the localization energy. In particular, the impact of annealing on the concentration of localized states, N_0, and/or on the localization length, α, of exciton center-of-mass in (GaIn) (NAs) QW's has been quantified. Comparison between simulation results and experimental data yields the annealing-induced reduction of the overlap parameter from $N_0\alpha^2 \simeq 1$ to $N_0\alpha^2 \lesssim 0.25$ for as-grown and annealed samples, respectively.

ACKNOWLEDGMENTS

[1] D. Gollub, S. Moses, and A. Forchel, IEEE J. Quantum Electron. **40**, 337 (2004).

[2] L. Grenouillet, C. Bru-Chevallier, G. Guillot, P. Gilet, P. Duvaut, C. Vannuffel, A. Million, and A. Chenevas-Paule, Appl. Phys. Lett. **76**, 2241 (2000).

[3] M. A. Pinault and E. Tournié, Appl. Phys. Lett. **78**, 1562 (2001).

[4] T. H. Chen, Y. S. Huang, D. Y. Lin, and K. K. Tiong, J. Appl. Phys. **96**, 6298 (2004).

[5] A. Hierro *et al.*, J. Appl. Phys. **94**, 2319 (2003).

[6] M. S. Skolnick, P. R. Tapster, S. J. Bass, A. D. Pitt, N. Apsley, and S. P. Aldred, Semicond. Sci. Technol. **1**, 29 (1986).

[7] S. T. Davey, E. G. Scott, B. Wakefield, and G. J. Davies, Semicond. Sci. Technol. **3**, 365 (1988).

[8] E. M. Daly, T. J. Glynn, J. D. Lambkin, L. Considine, and S. Walsh, Phys. Rev. B **52**, 4696 (1995).

[9] R. Zimmermann and E. Runge, Phys. Status Solidi A **164**, 511 (1997).

[10] S. D. Baranovskii, R. Eichmann, and P. Thomas, Phys. Rev. B **58**, 13081 (1998).

[11] H. Grüning *et al.*, Phys. Status Solidi C **1**, 109 (2004).

[12] B. Dal Don, K. Kohary, E. Tsitsishvili, H. Kalt, S. D. Baranovskii, and P. Thomas, Phys. Rev. B **69**, 045318 (2004).

[13] K. Kazlauskas, G. Tamulaitis, P. Pobedinskas, A. Zukauskas, M. Springis, C. Huang, Y. Cheng, and C. C. Yang, Phys. Rev. B **71**, 085306 (2005).

[14] A. Miller and E. Abrahams, Phys. Rev. **120**, 745 (1960).

[15] R. A. Mair, J. Y. Lin, H. X. Jiang, E. D. Jones, A. A. Allerman, and S. R. Kurtz, Appl. Phys. Lett. **76**, 188 (2000).

[16] A. Kaschner, T. Lüttgert, H. Born, A. Hoffmann, A. Y. Egorov, and H. Riechert, Appl. Phys. Lett. **78**, 1391 (2001).

[17] R. J. Potter and N. Balkan, J. Phys.: Condens. Matter **16**, S3387 (2004).

[18] H. D. Sun, A. H. Clark, H. Y. Liu, M. Hopkinson, S. Calvez, M. D. Dawson, Y. N. Qiu, and J. M. Rorison, Appl. Phys. Lett. **85**, 4013 (2004).

[19] H. F. Liu, C. S. Peng, E. M. Pavelescu, S. Karirinne, T. Jouhti, M. Valden, and M. Pessa, Appl. Phys. Lett. **82**, 2428 (2003).

[20] I. A. Buyanova, G. Pozina, P. N. Hai, N. Q. Thinh, J. P. Bergman, W. M. Chen, H. P. Xin, and C. W. Tu, Appl. Phys. Lett. **77**, 2325 (2000).

[21] M. Albrecht *et al.*, Appl. Phys. Lett. **81**, 2719 (2002).

[22] J. M. Chauveau, A. Trampert, K. H. Ploog, and E. Tournié, Appl. Phys. Lett. **84**, 2503 (2004).

[23] P. J. Klar *et al.*, Phys. Rev. B **64**, 121203 (2001).

[24] K. Volz, T. Torunski, B. Kunert, O. Rubel, S. Nau, S. Reinhard, and W. Stolz, J. Cryst. Growth **272**, 739 (2004).

[25] O. Rubel, K. Volz, T. Torunski, S. D. Baranovskii, F. Grosse, and W. Stolz, Appl. Phys. Lett. **85**, 5908 (2004).

[26] M. A. Pinault and E. Tournié, Solid-State Electron. **47**, 477 (2003).